AD-A064 897 NAVAL POSTGRADUATE SCHOOL MONTEREY CALIF F/G 11/6
VIBRATION ANALYSIS AND NONDESTRUCTIVE TESTING USING HOLOGRAPHIC--ETC(U)
DEC 78 P P HOFFMANN

UNCLASSIFIED NL

AD A064 897

END
DATE FILMED
4-79
DDC

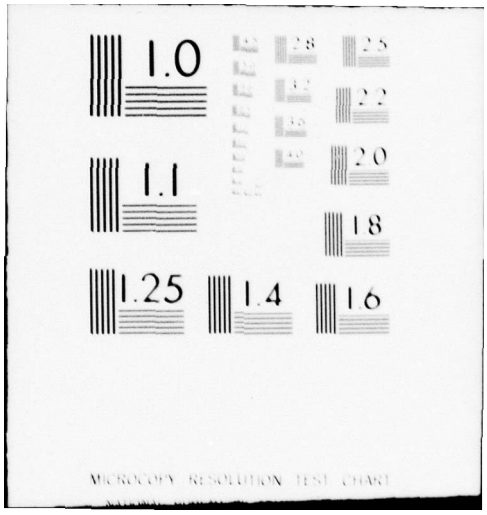
1.0
1.1
1.25
1.4
1.6
2.8
2.5
2.2
2.0
1.8
MICROCOPY RESOLUTION TEST CHART

NAVAL POSTGRADUATE SCHOOL
Monterey, California

THESIS

VIBRATION ANALYSIS AND NONDESTRUCTIVE TESTING USING HOLOGRAPHIC TECHNIQUES

by

Phillip P. Hoffmann

December 1978

Thesis Advisor: A. E. Fuhs

UNCLASSIFIED

SECURITY CLASSIFICATION OF THIS PAGE (When Data Entered)

REPORT DOCUMENTATION PAGE	READ INSTRUCTIONS BEFORE COMPLETING FORM
1. REPORT NUMBER	2. GOVT ACCESSION NO. 3. RECIPIENT'S CATALOG NUMBER
4. TITLE (and Subtitle) Vibration Analysis and Nondestructuve Testing Using Holographic Techniques.	5. TYPE OF REPORT & PERIOD COVERED Master's Thesis; December 1978
	6. PERFORMING ORG. REPORT NUMBER
7. AUTHOR(s) Phillip P. Hoffmann	8. CONTRACT OR GRANT NUMBER(s)
9. PERFORMING ORGANIZATION NAME AND ADDRESS Naval Postgraduate School Monterey, California 93940	10. PROGRAM ELEMENT, PROJECT, TASK AREA & WORK UNIT NUMBERS 12 76p.
11. CONTROLLING OFFICE NAME AND ADDRESS Naval Postgraduate School Monterey, California 93940	12. REPORT DATE December 1978
	13. NUMBER OF PAGES 75
14. MONITORING AGENCY NAME & ADDRESS(if different from Controlling Office)	15. SECURITY CLASS. (of this report) Unclassified
	15a. DECLASSIFICATION/DOWNGRADING SCHEDULE

16. DISTRIBUTION STATEMENT (of this Report)

Approved for public release; distribution unlimited.

17. DISTRIBUTION STATEMENT (of the abstract entered in Block 20, if different from Report)

18. SUPPLEMENTARY NOTES

19. KEY WORDS (Continue on reverse side if necessary and identify by block number)

Holography
Real-time Holograms
Vibration Analysis
Holographic Nondestructive Testing

20. ABSTRACT (Continue on reverse side if necessary and identify by block number)

Real-time holograms were made of Aluminum rectangular plates. The plates were cyclically vibrated with a piezo-electric driver to allow the fundamental frequencies to be measured and the mode shapes observed. These results were compared with theoretical frequency calculations.

The plates were flawed by three different methods, and real-time holograms were again made. The resonant frequencies

DD FORM 1 JAN 73 1473 EDITION OF 1 NOV 65 IS OBSOLETE S/N 0102-014-6601 |

UNCLASSIFIED

SECURITY CLASSIFICATION OF THIS PAGE (When Data Entered)

251 450

(20. ABSTRACT Continued)

of each plate were recorded, and each mode shape was observed.

A comparison between the plates before and after the flaws was made to determine the applicability of holography to the nondestructive testing of vibrating objects.

Results indicate that holographic nondestructive testing (HNDT) of vibrating objects shows great promise for future applications.

Approved for public release; distribution unlimited

VIBRATION ANALYSIS AND NONDESTRUCTIVE TESTING USING HOLOGRAPHIC TECHNIQUES

by

Phillip P. Hoffmann
Lieutenant, United States Navy
B.S., United States Naval Academy, 1973

Submitted in partial fulfillment of
the requirements for the degree of

MASTER OF SCIENCE IN MECHANICAL ENGINEERING

from the
NAVAL POSTGRADUATE SCHOOL
December 1978

Author Phillip P. Hoffmann

Approved by: Allen E Fuhs
Thesis Advisor

Paul J. Marto
Chairman, Department of Mechanical Engineering

William M. Tolles
Dean of Science and Engineering

ABSTRACT

Real-time holograms were made of Aluminum rectangular plates. The plates were cyclically vibrated with a piezoelectric driver to allow the fundamental frequencies to be measured and the mode shapes observed. These results were compared with theoretical frequency calculations.

The plates were flawed by three different methods, and real-time holograms were again made. The resonant frequencies of each plate were recorded, and each mode shape was observed.

A comparison between the plates before and after the flaws was made to determine the applicability of holography to the nondestructive testing of vibrating objects.

Results indicate that holographic nondestructive testing (HNDT) of vibrating objects shows great promise for future applications.

TABLE OF CONTENTS

LIST OF FIGURES

LIST OF TABLES

ACKNOWLEDGMENTS

The author would like to acknowledge the support of the Naval Postgraduate School Foundation, funded by the Office of Naval Research, for providing the equipment necessary to conduct this investigation.

I would also like to express my sincere appreciation to my thesis advisor, Dr. Allen E. Fuhs, for his excellent technical guidance and his patience. In addition, I would like to thank Mr. Roy F. Edwards for his prompt and sure assistance which enabled the project to run as smoothly as possible.

This thesis is dedicated to the memory of my late mother, Jean P. Hoffmann, who lost her two year battle with cancer just prior to its completion. Her courage and her love were constant sources of inspiration to me, throughout the course of this project.

I. INTRODUCTION

A. BACKGROUND

On December 4, 1964, the field of vibration analysis was suddenly and dramatically altered when the first hologram of a vibrating object was made. For the first time, humans could actually see and photograph the contours of vibration amplitudes. Since that time, the dreams and expectations of vibration analysts have been coming true. The techniques of holography are being used more and more by engineers for solving vibration problems.

The advantages of using holography for vibration analysis are many. By vibrating an object and making a hologram of it, the analyst is provided with a permanent record of that objects' vibration pattern and amplitude. In addition, unlike an interferometer, a hologram can be made of any diffusely reflecting, three dimensional object with a non-planer surface, rather than only an optically polished flat surface. This advantage is provided without sacrificing any of the interferometer's sensitivity or precision.

Holographic techniques also show a great deal of promise in the area of nondestructive testing. While the greater percentage of the work being done is in the field of optical holography, there is also holographic nondestructive testing being carried out in the fields of microwave and acoustic holography [7].

Holographic nondestructive testing (HNDT) using vibration techniques is commonly used in the testing of such things as turbine blades, thin wall castings, and blowers.

B. THESIS OBJECTIVE

The primary objective of this thesis was to learn and apply the techniques of optical holography to the vibrational analysis of plates. In addition, the applicability of using these techniques in the HNDT of plates was investigated.

II. EXPERIMENTAL METHODS

A. GENERAL

Dr. Denis Gabor invented holography thirty years ago while investigating ways to reduce spherical aberration in high-magnification electron microscopes. Stemming from the Greek root 'holos', which means whole, and the word gram, meaning message, a hologram is, in essence, a complete record of a scene or object. Holography, then, is the science of recording an entire optical wavefront on a suitable material, usually a photographic plate. Whereas a photograph records a three dimensional scene in two dimensions, a hologram captures and holds the true three dimensionality of a scene.

Unlike conventional photography, holography does not require the use of lenses. Instead, both phase and amplitude information are recorded as a result of the interference pattern formed when light waves are split and then rejoined after some portion has reflected off of the object desired. The portion of the beam which reflects off of the object and onto the plate is called the object beam. The remainder of the beam is transmitted directly to the photographic plate and is called the reference beam. Once recorded, the hologram itself will bear no resemblence to the recorded object. However, by illuminating the hologram in the same manner as it was originally exposed, the object may be viewed as if it were in its original position and will retain its three dimensionality. This process is called reconstruction.

In order to form high-contrast interference fringes on the photographic plate; that is, in order to make a good hologram, there are three distinct requirements which must be met.

1. Light Source Requirements

The light source used for holographic applications must exhibit long temporal coherence characteristics and must, therefore, be essentially a monochromatic source. Temporal coherence, most commonly expressed in units of length, is actually a measure in time of the phase consistency of successive wavefronts. The temporal coherence length is determined by multiplying the temporal coherence time by the speed of light, thus the units of length. Since the temporal coherence length of a light source is inversely proportional to the frequency bandwidth of the source, it follows that the longest lengths possible are achieved by monochromatic, or single frequency light sources. The laser, generally considered to be monochromatic, provides the best light source for holographic purposes. Figure 1 shows the laboratory warning used due to the lasers use.

Since the hologram is formed by the interference of two light waves converging on the photographic plate, the temporal coherence length is an extremely important factor. For optimum high-contrast holograms, the path lengths of the object and reference beams must be as nearly equal as possible. With an extended temporal coherence length, such

as with the laser, these paths may vary as much as a couple of inches. With a standard light source, on the other hand, the beams would have to be matched within microns.

2. Vibration Stability Requirements

Holography is essentially the recording of interferometric fringes on a photographic plate. In order to accurately record the phase and amplitude of the desired object, it is necessary to maintain a high degree of vibrational stability. Otherwise, unwanted interference fringes might occur. In fact, in order to be assured of high contrast holograms, the equipment must be stable to within a fraction of the wavelength of the light source used.

3. Photographic Plate Requirements

Due to the fact that the two beams utilized to form the interference fringes arrive from different directions, forming the so-called offset angle, the fringe frequency recorded by the photographic emulsion is extremely high. When recording these dimensional scenes, additional increases in frequency occur. Plates or films with extremely high resolution are, therefore, required. In order to calculate the plate resolution which is required, the fringe frequency can be determined from the following:

$$\nu \simeq [2 \sin (\theta/2)]/\lambda \qquad (1)$$

where θ is the offset angle and λ is the wavelength of the

light source [Ref. 7]. For example, using the above equation, it can be determined that a hologram taken with a Helium-Neon laser (632.8 nm wavelength), with an offset angle of 45 degrees, requires a plate resolution in excess of 1200 lines per millimeter.

B. TECHNIQUES OF INTERFEROMETRIC HOLOGRAPHY

Since a hologram of an object records its phase and amplitude on the order of wavelengths, holographic techniques are extremely well suited to non-destructive testing applications. There are three different types of holograms which are particularly well suited to this use.

1. Real-Time Holography

This method consists of taking a single exposure of a static object. The hologram is then developed and replaced in its original position. Since it must be replaced within a fraction of a wavelength of its original position, developing tanks which allow in-place processing are commonly used for this type of holography. When reconstructed with the original reference and object beams, the holographic image will be superimposed on the original object. If the object is then displaced slightly, interference fringes can be observed at the instant that they occur – hence the name Real-Time holography. The outstanding advantage to this type of hologram is that numerous different kinds of movements can be studied with a single holographic exposure. Unfortunately, fringe contrast and sensitivity are generally

reduced when using this technique to study vibratory motion. The time saving and flexibility which are provided by this method, however, generally outweighs these disadvantages.

2. Time-Average Holography

This method consists of taking a single exposure hologram of an object while it is undergoing cyclic vibratory motion. Due to the nature of vibratory motion, that is, the fact that an object subjected to this type of motion will spend the greatest percentage of time at its displacement extremes, a hologram will record interference fringes corresponding to the position of the object at its largest displacement. That is provided, of course, that the exposure time is long compared to one period of the vibration cycle. This technique is a valuable tool in the study of one specific vibration mode of a test specimen. A time average hologram permanently stores information about the amplitude of vibration and location of vibratory nodes.

3. Double-Exposure Holography

This method consists of one exposure of an object, displacing the object, and then exposing the same photographic plate once again. When the hologram is processed and reconstructed, it will display the interference pattern caused by the displacement of the object which occurred between exposures. This is an excellent technique for studying objects which have undergone static loading such as beams or pressurized pipes. A complete description of this

technique applied to the nondestructive testing of pipes is contained in [8].

III. EXPERIMENTAL PROCEDURE

A. HOLOGRAPHIC SYSTEM

The components of the holographic system used can be grouped into three distinct areas: first, the holographic equipment utilized to produce holograms in general; second, the vibration equipment utilized for this specific investigation; and third, the photographic plates and their development system which enables in-place processing to be accomplished.

1. Holographic Components

The foundation for all of the optical components and the test specimens is a vibration isolation table which is supported by four vibration isolation mounts located in the legs. The table, which has a honeycomb stainless steel top drilled and tapped with 1/4-20 mounting holes on one-inch centers, weighs approximately 1000 pounds. It floats on air bags, pressurized with a regulated supply of nitrogen, which are installed in each leg. Automatic leveling is accomplished by regulators which control the nitrogen flow to each leg and respond to any excitation causing movement of the table. The table with the optical components in place is pictured in Figure 2.

The optical components of the holographic system and their functions are described below. Their position on the table is schematically depicted in Figure 3.

1) LASER: provides the coherent and monochromatic light source. A 10 milliwatt, Hughes model 3170H, Helium-Neon laser with a 5 millimeter beam was utilized.

2) BEAM STEERER: provides the horizontal and vertical beam steering capability necessary to direct the beam along the proper path after it leaves the laser. A JODON BA-500A Beam Steerer was utilized in these experiments.

3) LASER SHUTTER: provides photographic plate exposure control with shutter speeds variable from T to 125^{th} of a second. A JODON S-10B Laser Shutter was utilized.

4) VARIABLE BEAM SPLITTER: provides a continuously variable beam splitting capability which splits the laser beam into the object and reference beams and enables fine adjustment of beam intensities at the photographic plate. The JODON VBA-200 Variable Beam Splitter utilized is pictured in Figure 4a.

5) MIRROR POSITIONERS: provide a precise beam positioning capability and enable equal path lengths to be achieved. One of the three JODON MH-50 Mirror Positioners user is pictured in Figure 4b.

6) MIRROR MOUNT: provides the same service as mirror positioners, however, has no fine adjustment capability. A RM-45 JODON Mirror Mount was utilized.

7) LENS PINHOLE SPATIAL FILER (consisting of a microscopic objective and pinhole mounted on a magnetic base): remove irregularities in the beam due to imperfections

or dirt on the beam splitter or mirrors. In addition they expand the object and reference beams just prior to their arrivals at the object and photographic plate respectively. One of the two JODON LPSF-100 Spatial Filters used is pictured in Figure 4c. For the object beam, a pinhole size of 50 microns was used with a microscope objective of 20 x 0.40. For the reference beam, a pinhole size of 25 microns was used with a microscope objective of 20 x 0.40.

In addition to these components, a light meter was used to measure the respective intensities of the object and reference beams. It consisted of a planar diffused silicon PIN photodiode connected to a digital voltmeter. This device, used in conjunction with the variable beam splitter, enables the beam intensities to be accurately matched at the photographic plate.

2. Vibration Equipment

In order to provide the excitation required to displace the test specimen, an electronic shaker was utilized. The shaker, which incorporates a PZT transducer to induce mechanical motion, was driven by an audio oscillator. Since the displacement of the shaker is directly proportional to the input voltage, at the rate of 0.12 microns per 100 volts, the signal from the oscillator was stepped up through a power amplifier and transformer. The signal was then fed through a voltmeter before entering the shaker. This arrangement allowed for a larger range of shaker displacements and enabled

these displacements to be easily monitored. A digital frequency counter was also connected to the oscillator to increase the accuracy of frequency read-outs. The shaker which was utilized, a JODON EV-30, is pictured in Figure 5.

3. Photographic Plate/Development System

a. Photographic Plates: The photographic plates used were standard KODAK plates specifically designed for use in holographic research. Designated 131-02, these are exceptionally fast when exposed with Helium-Neon lasers and meet the resolution requirement outlined in Chapter 2.

b. Development System: The development system, pictured in Figures 6 and 7, consists of a holding tank to allow in-place processing, 5 aspirator bottles containing the processing fluids, and a network of tubing providing flow from the bottles to the tank. A valve manifold enables each chemical to be run into the tank and a pump is used to provide agitation. Following the stipulated rinsing times, chemicals are drained from the tank to bottles on the floor for re-use.

B. TEST SPECIMEN SELECTION

Three questions had to be answered before the actual test specimens could be selected. What material should the specimens be made from? What shape should they be? What size should they be?

1. Material Selection

The selection of the specific material for use as test specimens was made with consideration being given to

two primary requirements. The material chosen had to be a metal commonly used for Naval applications and have a low damping capacity.

In order to better understand the damping requirement, consider that an excited metal plate vibrates in much the same way as a mass-spring-damper system in parallel. The greater the damping inherent in the plate material, the greater the width of the resonant peak in the response curve. Figure 8 displays graphically the differences in response curves for typical high and low damped systems.

The resonant frequency in each case occurs at the response peak. In order to observe a resonant frequency shift due to a cut in the plates, a minimum peak width is highly desirable. If Δf_d is the width of the resonant frequency peak and Δf_c is the change in resonant frequency due to the cut, then Δf_c must be much larger than Δf_d in order to be able to isolate a frequency change due to the cut. Once the requirements for a low damped material was established, a method of quantifying material damping was sought.

One method of measuring the damping capability of a material which is commonly used is the specific damping capacity (SDC). This measure is derived from the decay of free oscillation of an excited bar specimen as shown in Figure 9. The SDC is then calculated from

$$SDC = \frac{(A_n - A_{n+1})^2}{A_n^2} \times 100\% \qquad (2)$$

This relationship, which directly relates absorbed energy to the square of the amplitude, enables materials to be tabulated according to their damping capabilities. Table 1 lists some common structural materials and their SDC's.

Based on the two requirements stipulated above for this investigation, alluminum alloy 2024-T4 was chosen as the test specimen material.

2. Specimen Shape

In order to be able to carry out the investigation with the best possible chance for meaningful results, a shape must be chosen for which there exists a great deal of theoretical information. In addition, the physical application of boundary conditions must be realistically feasible on the shape chosen. An all-sides-clamped configuration was chosen to satisfy the latter of these two requirements. This decision ensures that the greatest possible accuracy will be obtained while physically satisfying the boundary conditions in the laboratory. Three shapes were then considered for the plates: circular, square, and rectangular.

Considerable theoretical information on the vibration of circular plates can be found in references [10,11]. However, the complications involved with constructing a specimen mount made this choice undesirable.

The square plate at first appeared to be an excellent choice; however, further research exposed an interesting phenomenon which occurs in the case of a vibrating square

plate. This condition, called degeneracy, occurs when the allowed frequencies become equal in pairs due to the equal length of sides. When the degeneracy occurs, an infinite number of mode shapes may appear at the same frequency. In order to avoid the frustration of coping with this condition, the square plate was also rejected.

Rectangular plates were then considered for the test specimens. These were ultimately chosen for several reasons. They lend themselves well to laboratory mounting, extensive theoretical information on vibrating rectangular plates is available [10], and special complications are not involved in isolating a specific resonant frequency or mode shape.

3. Specimen Size

The exact size of the plate was carefully chosen with consideration being given to three specific constraints. First, the area of the plate had to be compatible with the capability of the available holographic equipment. Second, the length of the sides was further constrained by the fact that the available tabular data on frequency parameters was limited to specific side length ratios. Third, the thickness was also an important decision because it figures prominently in the calculation of flexural rigidity which is a major contributor in the theoretical determination of fundamental frequencies. Bearing each of these constraints in mind, a rectangular plate six by four inches on the sides, with a thickness of twenty thousandths of an inch was chosen. One of the plates used is shown in Figure 10.

C. THEORETICAL FREQUENCY DETERMINATION

Once the material and shape and exact size of the test specimens had been selected, calculations were made to determine the expected frequencies for each of the mode shapes. The frequency parameters, f_n, for an all-sides-clamped rectangular plate are given as

$$f_n = \omega_n b^2 \sqrt{\rho/D} \tag{3}$$

where

ω_n = circular frequency of the n^{th} mode in radians/second

b = length of shorter side in feet

ρ = density in slugs/foot squared

D = flexural rigidity in foot-pounds

n = number of mode

The flexural rigidity is defined as

$$D = \frac{Eh^3}{12(1 - \nu^2)} \tag{4}$$

where

E = Young's modulus in psi

h = plate thickness in inches

ν = Poisson's Ratio

For the aluminum alloy 2024 plates which were used, values of the physical constants are:

$$E = 10 \times 10^6 \text{ psi}$$

$$\nu = 0.33$$

$$h = 0.020 \text{ inches}$$

This gives a flexural rigidity of

$$D = 0.6234 \text{ ft-lbf}$$

Further, for an aluminum alloy 2024 plate 0.020 inches thick

$$\rho = 0.008723 \text{ slugs/ft}^2$$

Therefore,

$$\sqrt{\rho/D} = 0.11828 \text{ sec/ft}^2$$

Then, from [10], for a rectangular plate with a side length ratio of 1.5, the frequency parameters, f_n, are:

$$f_1 = 27.00$$

$$f_2 = 67.58$$

$$f_3 = 81.57$$

The fundamental frequencies are calculated to be:

$$\omega_1 = 326.975 \text{ Hz}$$
$$\omega_2 = 818.407 \text{ Hz}$$
$$\omega_3 = 987.829 \text{ Hz}$$

D. TEST SPECIMEN MOUNT

In order to support the aluminum plates in such a way to permit testing in accordance with the experimental methods, a mount had to be designed and built. Due to the nature of the experiment, several factors had to be taken into account during the design phase.

1. Boundary Conditions

Since test specimen selection and subsequent theoretical frequency calculations were based on a rectangular plate, clamped on all sides, care had to be taken to assure that this boundary condition was satisfied to the fullest degree possible.

2. Shaker Mount

Since exact frequency measurements were to be taken, it was necessary to assure that the shaker was securely mounted in order to eliminate the inaccuracies inherent with a moving shaker.

3. Table Isolation

Due to the nature of holography and the importance of table stability, as outlined in Chapter 2A, the mount had to be constructed in such a way that vibration was not

transmitted to the holographic table. The mount designed was further isolated from the table by a large piece of heavy foam rubber. This piece of foam rubber was later found to be unacceptable because it did not allow the mount to be firmly attached to the table.

The specimen mount designed and built to meet these specifications is shown in Figure 5.

E. TEST PROCEDURE

1. Making a Hologram

a. Preparing for Exposure

In order to arrange the equipment to make a good hologram, the following steps must be taken. To begin with, the optical components and object must be aligned so that the path lengths of the reference and object beams are nearly equal. This will ensure that the temporal coherence length provided by the laser will be enough to result in high-contrast interference fringes. In practice, these lengths were adjusted within an inch of each other. Once this has been accomplished, the table should be activated to provide the necessary vibration isolation. Now, the laser should be turned on to allow the optical components to be aligned so that the two beams are illuminating the object and the plate. The photodiode is activated and placed behind the plate holder in a position where it bisects the offset angle between the object and reference beams. The beam splitter is then adjusted until the

intensities of the respective beams are essentially equal. Finally, the photodiode is removed from the table and the shutter is placed between the beam steerer and the beam splitter. The shutter speed should also be set at this time based on the combined intensities of the object and reference beams reaching the plate. Though there is a certain amount of trial and error involved with selecting the proper shutter speed, as a general guideline, the following combinations were successfully utilized with the 131-02 KODAK High Speed Holographic Plate. With a combined beam intensity of approximately 0.0400 volts, an exposure of 1/2 of a second should be utilized. Likewise, with a combined intensity of 0.0800 volts, an exposure of 1/4 of a second is required. It should be noted that in spite of the linearity apparent in these two examples, the relationship between intensity and exposure time is not a linear one.

b. Exposing the Plate

After the previously described set up procedures have been followed, the holographic plate is ready to be exposed. With the laser turned off and with the room in total darkness, the plate may be removed from its box and carefully placed in the holding/developing tank. The plate box is then carefully re-covered to avoid exposing any other plates. Next, the laser should be turned on, the shutter released, and the laser turned off. This process must be carried out smartly to avoid any excess laser radiation

from affecting the exposure. Once the plate has been exposed, the light-tight cover is placed over the developing tank. When this has been accomplished, the room lights may be turned back on.

c. Developing the Plate

After the exposure, the processing of the 131-02 holographic plate must be performed in the following manner, as recommended by KODAK.

(1) Open the valve allowing the D-19 developing solution to fill the tank. As soon as this valve is opened, begin a seven minute timer. When the tank is filled, close the valve and turn on the pump causing the agitation of the tank's contents. When seven minutes time has passed, open the drain valve and secure the pump.

(2) Open the valve allowing the tank to fill with KODAK INDICATOR STOP BATH. When the tank is full, activate the pump for a period of 15 seconds. Then secure the pump and drain the tank.

(3) Open the valve allowing the KODAK FIXER to fill the tank. Start a seven minute timer when the valve is opened. Once again, pump when the tank is full and secure/drain at the end of seven minutes time.

(4) Repeat step #3 with distilled water.

(5) Repeat step #3 with one part methanol and one part water. This rinse is required to remove a high level of residual sensitizing dye from the emulsion. This

dye is distinctly blue and experience may dictate a lesser rinse time for the removal of this color. [Two parts ethanol and one part water may also be used.]

(6) Finally, wash in distilled water again for a period of six minutes.

When the final wash has been completed, the hologram should be allowed to air dry in place. After drying is complete, the hologram is ready to be reconstructed.

d. Reconstructing the Hologram

In order to reconstruct a Time-Average or Double-Exposure hologram, the original reference beam alone must be shined on the plate. Then, by looking back through the hologram in the direction of the original object the reconstruction of the object will be clearly visible. Any fringes which are visible due to the displacement of the object are a permanent part of the hologram, so it is not necessary to maintain the photographic plate in its exact position for reconstruction. The intensity of the reference beam may be adjusted to vary the brightness of the reconstructed image.

The reconstructed image may then be photographed providing the experimenter with a permanent record which can be viewed or studied without the aid of the laser. Any high speed film can be used to accomplish this, however, two films in particular are excellent for use with

red-emitting lasers. Kodak Technical Pan SO-115 is a 35 mm film manufactured specifically for use in holographic reconstruction. Polaroid 57 high speed film is also an excellent reconstruction film. Since Polaroid 57 also has the added advantage of on-the-spot developing, enabling the photographer to make immediate f-stop and shutter speed corrections, it was used for the reconstruction photographs in this thesis. When photographing a hologram, it is important to note that the camera should be focused on the spot where the object was originally located and not on the photographic plate.

In the case of Real-Time holography the process is somewhat different. Once again the reference beam alone will produce a reconstructed image of the object. In order to observe the Real-Time phenomenon, however, the original object beam must also be activated. Then, provided that the plate and object are in exactly their original positions, the reconstructed image will appear superimposed on the actual object as desired. The beam splitter should then be adjusted so that the object and its reconstructed image appear equal in intentisy. When that has been accomplished, excitation of the object will cause the real-time fringes which may be seen when viewing the object through the hologram. During excitation, the fringes are visible, and the reconstruction may be photographed.

2. Holographic Techniques Utilized

a. Initial Attempts

Due to the advantages outlined in Chapter II.B.L, that is, the time saved and flexibility inherent in the Real-Time holography method, this technique was selected as the experimental method to be utilized.

To begin with, several attempts were made to make a hologram of a stationary plate. This in itself was easier said than done, however, and it was not until the tenth exposure that a successful hologram was actually made. While attempting to make that first successful hologram, a frustrating trial and error system was utilized. The steps outlined in Chapter III.E.1 were carefully followed for each exposure with various shutter speeds and developing times. In the end, however, the problem was defective Kodak D-19 developing solution. Extreme care must be taken when mixing the processing solutions to ensure that the manufacturer's directions are followed explicitly.

During the early attempts to make a hologram, two tests were discovered which can be conducted before the entire developing process is completed. If the plate fails either of these tests, it is not a usable hologram, and the remainder of the processing may be discontinued. The first test is carried out just after completion of the fixing process. When the Kodak Fixer has been drained

from the developing tank and replaced with distilled water, the light-tight cover may be removed. Once this has been done, the photographic plate should be observed. It should appear light blue in color and should be clear enough to see through. If the plate is too dense to see through, with the room lights on, then it will not be a useful hologram. The second test may be given after the final water wash has been drained from the tank. With the reference beam turned on, the plate should be viewed in the direction of the oncoming beam. As a result of diffraction, several red dots in a horizontal line should be evident. If there is only one red dot, the plate is not a hologram and need not be dried.

Once the ability to make holograms had been mastered, the center of the test plate was bolted to the piezoelectric shaker, and the first attempt at Real-Time vibration analysis was made. The reconstruction of this hologram produced an interesting result. When illuminated with the reference beam alone, the plate exhibited fringes. This reconstruction is pictured in Figure 12. Unfortunately, when the object beam was also utilized and the shaker activated there was no apparent change in the fringes. Subsequent holograms produced similar results.

At this time the lack of vibration fringes was attributed to the electronic shaker. In order to ascertain the validity of this assumption, the test mount was removed and a hologram was made of a car radio speaker which was

painted silver. When the speaker was wired to the audio oscillator, it was obviously vibrating, so fringes were expected. The speaker was placed in a heavy vice and positioned on the table. The hologram pictured in Figure 13 was then made and, upon completion, reconstructed. Then the oscillator was activated and the speaker observed. Fringes were created; however, the fringes were off center and disappeared at high vibration amplitudes. While further attempts to produce the desired fringes were being made, the vice holding the speaker was inadvertantly tapped. This resulted in the fringes shown in Figure 14. A slightly harder tap caused the fringes to disappear and no manner of excitation could produce any other fringes. This result provided the key to solving the previously experienced problems with the plate. Evidently, the two images were no longer exactly superimposed on one another. If a light tap was enough to move the heavy vice too much, then surely the specimen mount, which was sitting on a foam rubber pad, was not anchored sufficiently.

The mount was therefore modified for mounting in vices which were bolted to the table. The first hologram made with this new arrangement netted the best results to date. No fringes were evident when the hologram was reconstructed using the reference beam alone. This indicated that the holograms made while the mount was sitting on the foam rubber, such as Figure 12, were

actually Time-Average holograms, since movement must have occurred during exposure. Unfortunately, the fringes shown in Figure 15 occurred upon superposition. Extra care was taken during the processing of subsequent holograms to avoid touching the table unless it was absolutely necessary. This measure minimized the problem of superposition fringes enough to enable the production of usable vibration fringes.

b. Pre-Flaw Holograms

After the problems outlined above had finally been solved, a Real-Time Hologram of the test plate was made. With holographic reconstruction and shaker activation, the different vibration modes could be seen clearly as the frequency was varied at the audio oscillator. Each mode was carefully dialed in to view and the resonant frequency was recorded. The second and fourth modes were recorded on Polaroid film and are pictured in Figures 16 and 17 respectively.

c. Post-Flaw Holograms

(1) Diagonal Slit

The first flow introduced in the plate was a diagonal slit, approximately 1/2 inch long and 1/32 of an inch wide, located in the upper left hand quadrant of the plate. The slit was placed diagonally on a line between the center of the plate and the upper left hand corner. A Real-Time hologram was then made of

the flawed plate. Once again, reconstruction and excitation caused vibration fringes to appear. Mode shapes were observed and resonant frequencies were recorded. The second vibration mode of the flawed plate is pictured in Figure 18.

(2) Vertical Slit

Next a vertical slit was cut into a test plate. This slit was carefully cut to exact dimensions and placed parallel to the left hand edge of the plate half way between the edge and the center. The slit was one inch long and 0.050 inches thick. Again the Real-Time hologram was made, mode shapes observed and resonant frequencies recorded. Figures 19 and 20 show these mode shapes.

(3) Hole

Next a 0.125 inch diameter hole was drilled in a test plate. The hole was placed exactly half way between the center and left hand edge of the plate and was also centered vertically. Refer to Figure 21 for orientation of the plate. The plate with the hole was then holographed and studied as previously done with the other samples.

IV. EXPERIMENTAL RESULTS

A. PRE-FLAW

The reconstructed hologram of the test plate provided the basis for an excellent Real-Time vibration analysis. As the input frequency from the audio oscillator was varied, the different mode shapes could be seen clearly. It was extremely easy to dial in each of the plate's resonant frequencies by watching each mode shape come into view. Once each mode shape was isolated, its resonant frequency was recorded. The measured frequency of the first mode was 380.1 Hz, the second 630.8 Hz, and the fourth 987.6 Hz.

B. POST-FLAW

1. Diagonal Slit

When the original test plate was flawed with a diagonal slit and then re-holographed, its reconstruction displayed a definite change in the vibration pattern. This was particularly obvious in the second vibration mode, pictured in Figure 18. The fringes on the left side of the plate have obviously been altered when compared to those in Figure 16, the same plate vibrating in the second mode before the flaw had been introduced. The resonant frequencies were also altered. In the second mode the resonant frequency was 615.1 Hz and in the fourth 936.3 Hz. In

both cases, these were significant downward shifts in the resonant frequencies as compared to the pre-flaw plate.

2. Vertical Slit

The Real-Time hologram of the test plate flawed with the vertical slit revealed the most dramatic results. In effect, the plate had been "cut in half" by the flaw. In Figure 19, the plate is pictured with the right half vibrating in the second mode at 563.2 Hz. The left half of the plate, however, is not resonating. Figure 20 shows the same plate with the flawed, or left half, vibrating at its second mode resonant frequency. This picture was taken at a frequency of 510.1 Hz.

3. Hole

The small hole drilled in the left half of the test plate also caused a change in the mode shapes and fundamental frequencies, however, the effect was less dramatic. The second mode frequency was 588.8 Hz and the fourth mode was 903.5 Hz. Figure 21 shows the fourth mode shape of this plate.

All of the experimental results are tabulated in Table II.

C. EVALUATION OF RESULTS

1. Measured vs. Theoretical

Comparison between the experimental and theoretical resonant frequencies would appear to be favorable, expecially in the first mode. Unfortunately, even though great care

was taken to meet boundary conditions, this concern was somewhat negated when the center of the plate was bolted to the shaker. With the hole in the center of the plate and the relatively large area of excitation used, any comparison with the pure plate theory would be meaningless. In spite of the modifications which were made in the plate, however, the pure plate theory provided an excellent rough estimate of the actual plate frequencies. Table II shows data which confirm this observation. For a summary of the theoretical work which would be involved in determining the resonant frequencies of the bolted plate, refer to Appendix A.

2. Pre-Flaw vs. Post-Flaw

In each test case the resonant frequencies of the flawed plates were significantly lower than those of the plate before the flaw was introduced. The most dramatic frequency decreases being those in the plate with the largest flaw, in this case the vertical slit. The frequency shifts ranged from a decrease of 2.5%, in the second mode of the diagonal slit, to 10.7% in the second mode of the vertical slit.

In addition, the mode shapes were noticeably changed in each case providing visual evidence of the flaws. This phenomenon is most apparent in Figures 20 and 21.

V. CONCLUSIONS

Three definite conclusions can be drawn from the results of this experiment.

1. A flaw in a rectangular plate clamped on all sides gives rise to a significant resonant frequency shift when the plate is excited with a cyclic vibratory motion.

2. This shift in resonance frequency is always a decrease when compared to the unflawed plate frequencies.

3. When compared with the undamaged plate, a change in the vibration mode shapes is visually apparent in the immediate vicinity of the flaw.

These results indicate conclusively that holography provides the engineer with an interest in vibration, with an excellent method for observing first hand the response of an object to cyclic excitation. Once mastered, it is a relatively easy process, and the results are exceptionally useful. The minutest motions can actually be seen and studied with the naked eye. Still photographs and even movies can be made of an object in vibratory motion. Clearly, holography is an invaluable tool in the field of vibration analysis and can only continue to grow and expand in time.

As far as the field of holographic nondestructive testing is concerned, the results of this experiment indicate that HNDT using vibration techniques is an excellent method for discovering or detecting flaws in test specimens. Once the resonant frequencies and mode

shapes of a good object are known, similar objects may be tested for flaws by making a resonant frequency comparison or by detecting changes in mode shapes.

The complications and complexities of real-time holography, however, appear to make its application outside of a strict laboratory environment extremely limited. Time-average holography, on the other hand, while not as flexible, is a much easier technique and should find its way out of the laboratory sooner. The dramatic results with, and capabilities of, holography indicate a brighter future for this method of NDT and warrant extensive further research in this field.

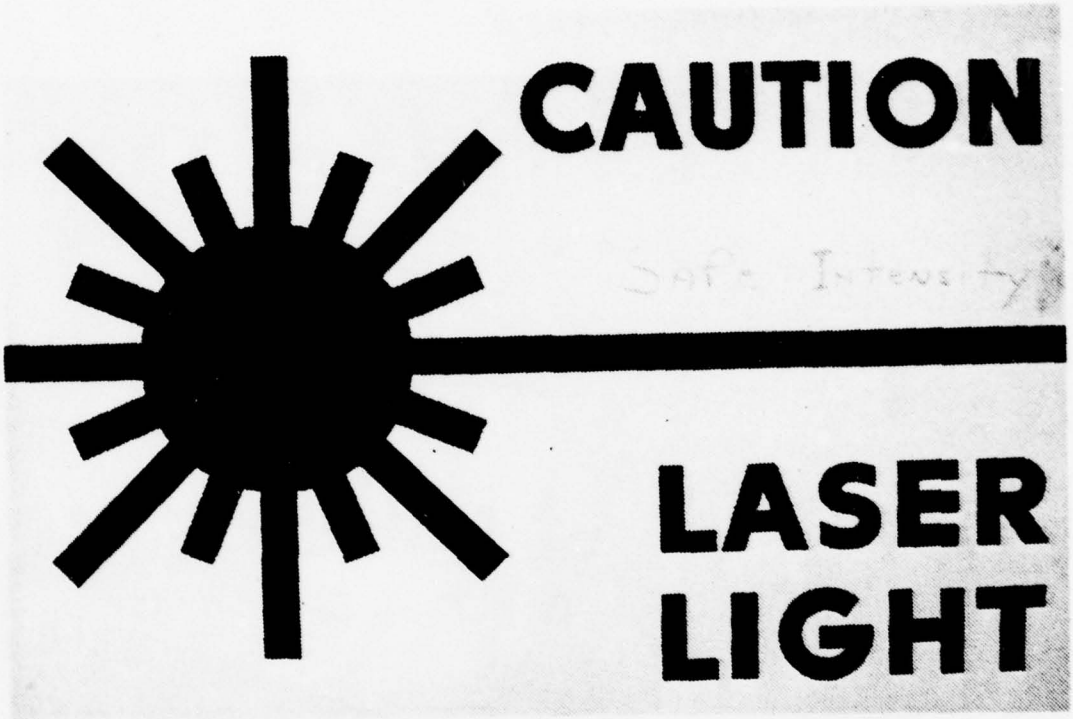

FIGURE 1. Laboratory Entrance Warning

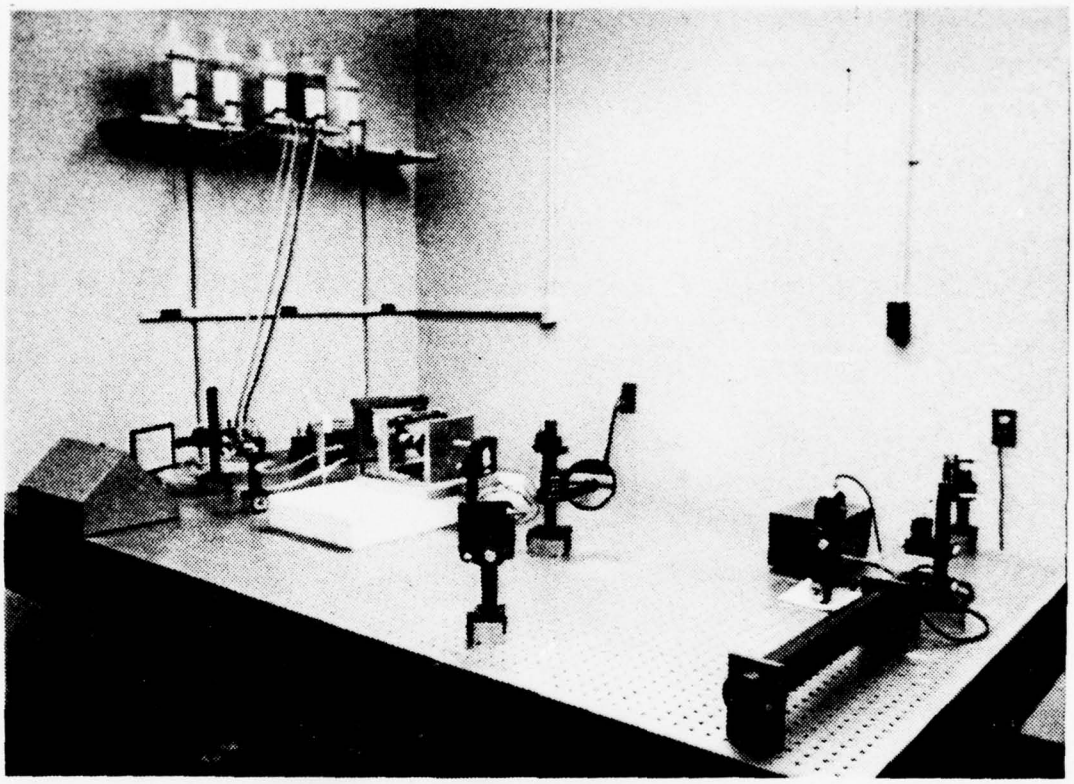

FIGURE 2. Vibration Isolation Table with Laser, Optical Components, and Test Specimen in Place

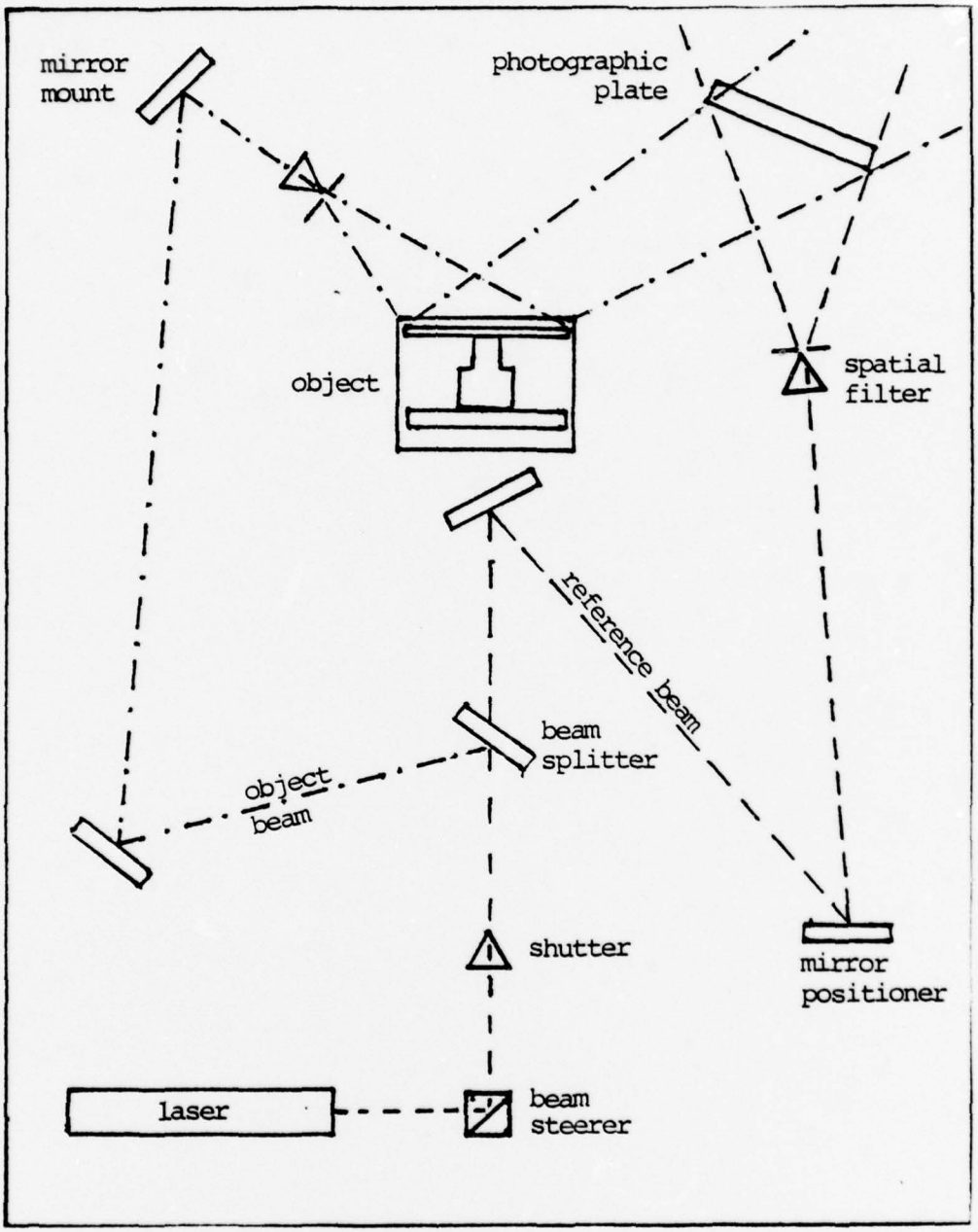

FIGURE 3. Schematic Diagram of Holographic System Layout

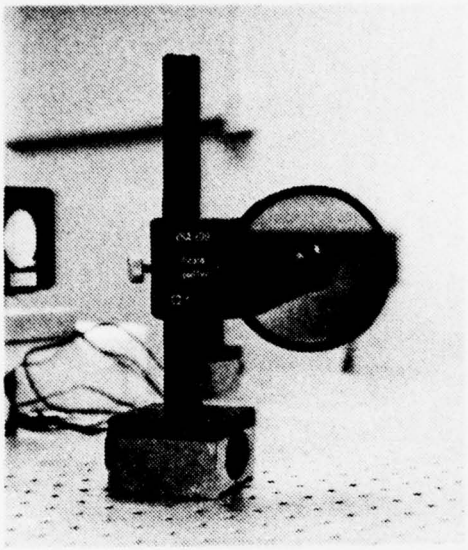

a) Variable Beam Splitter
(Jodon VBA-200)

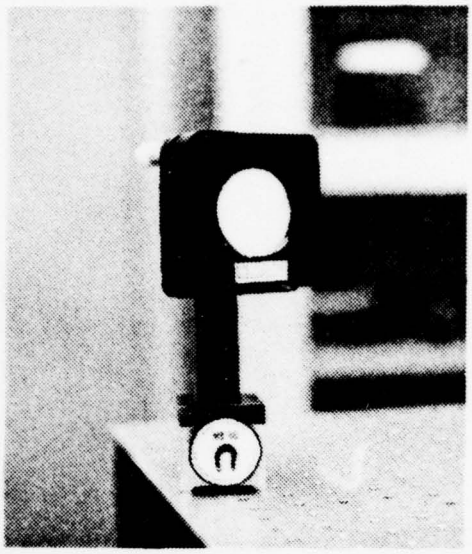

b) Mirror Positioner
(Jodon MH-50)

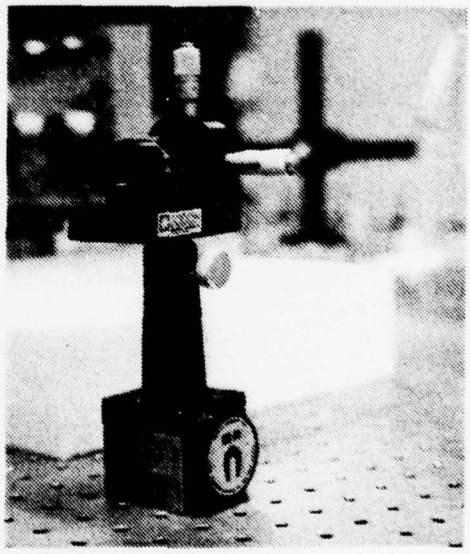

c) Lens Pinhole Spatial Filter
(Jodon LPSF-100)

FIGURE 4. Holographic Optical Components

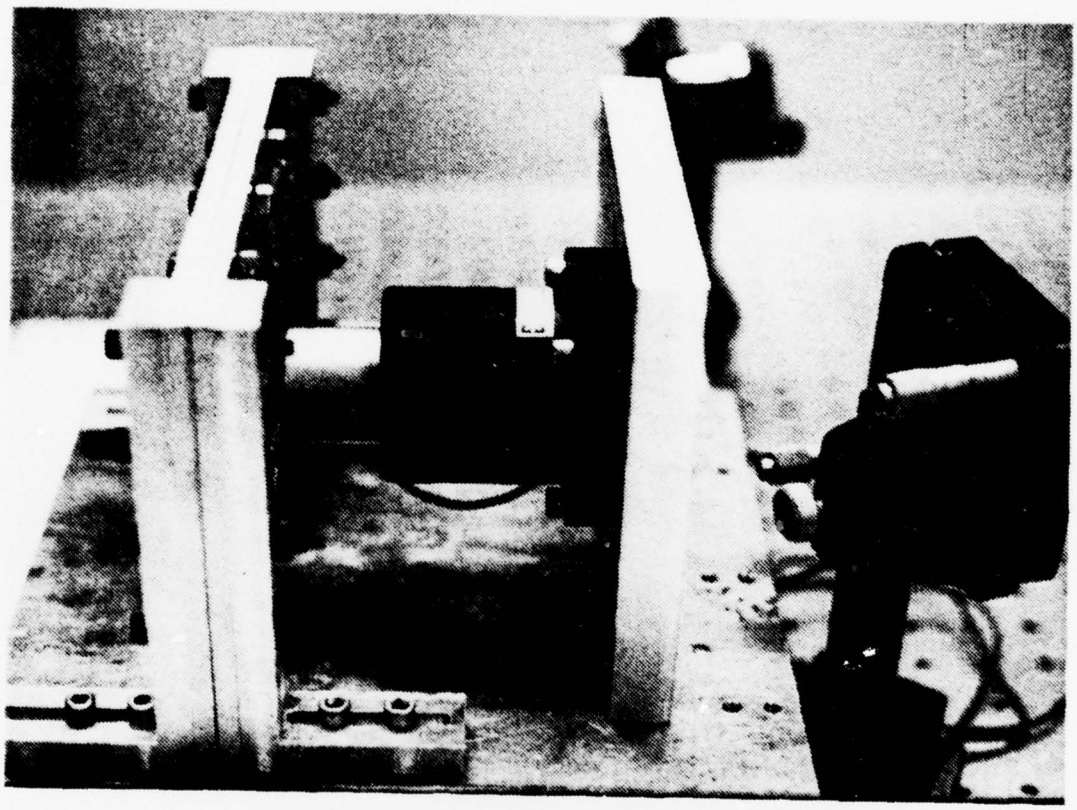

FIGURE 5. Electronic Shaker/Test Specimen Mount

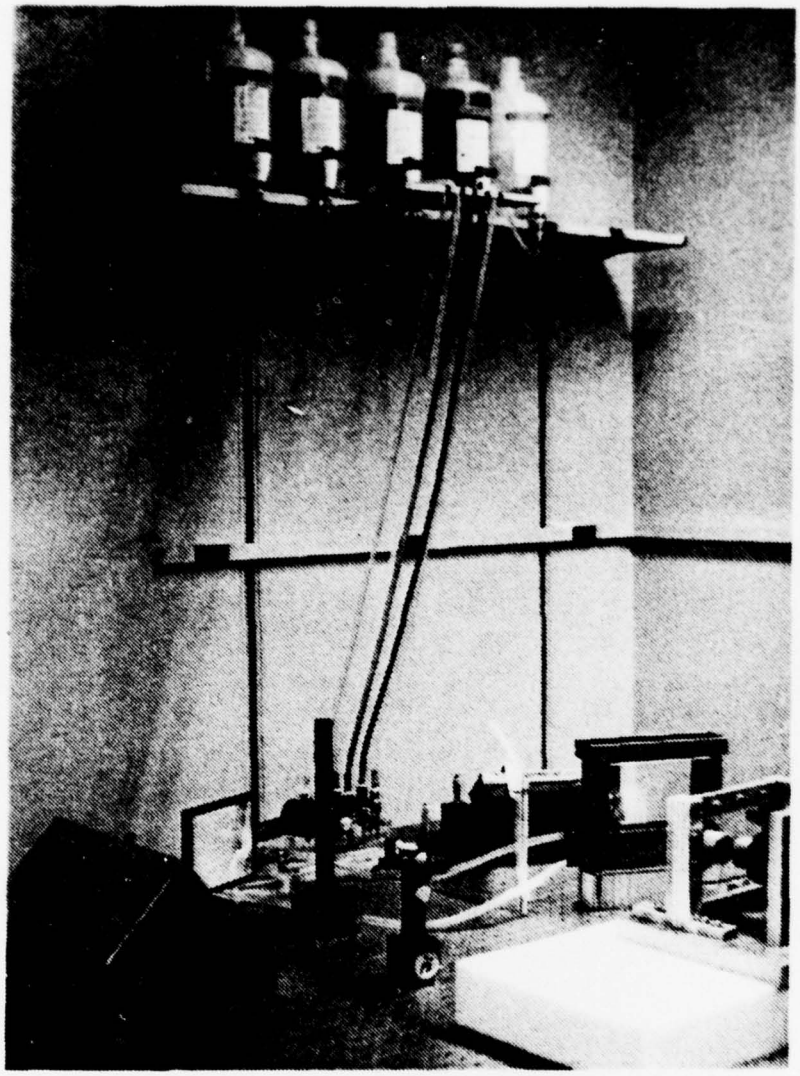

FIGURE 6. Photographic Plate Development System

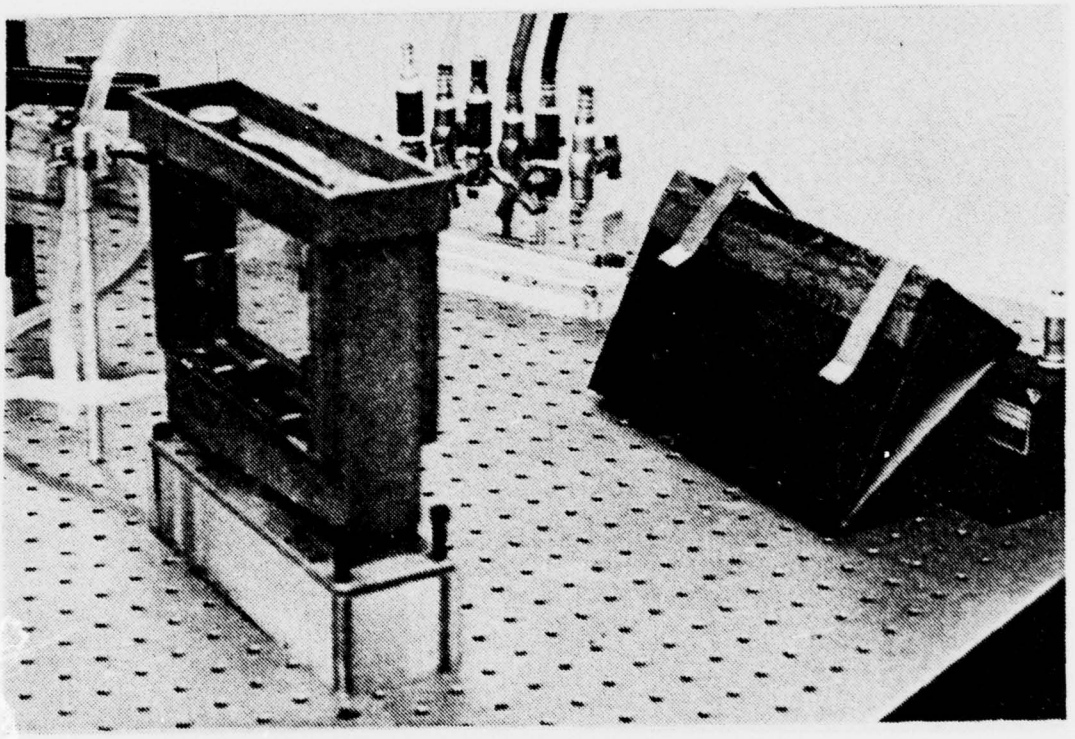

FIGURE 7. Photographic Plate Holder/Developing Tank and Valve Manifold

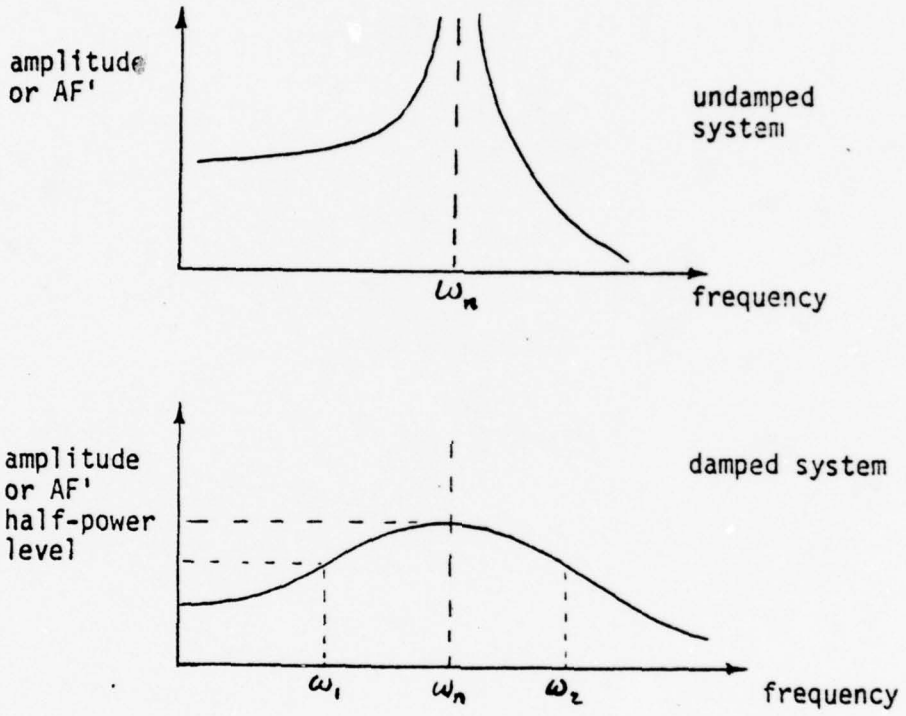

FIGURE 8. Influence of Damping on Response
(Reproduced from Edwards [6])

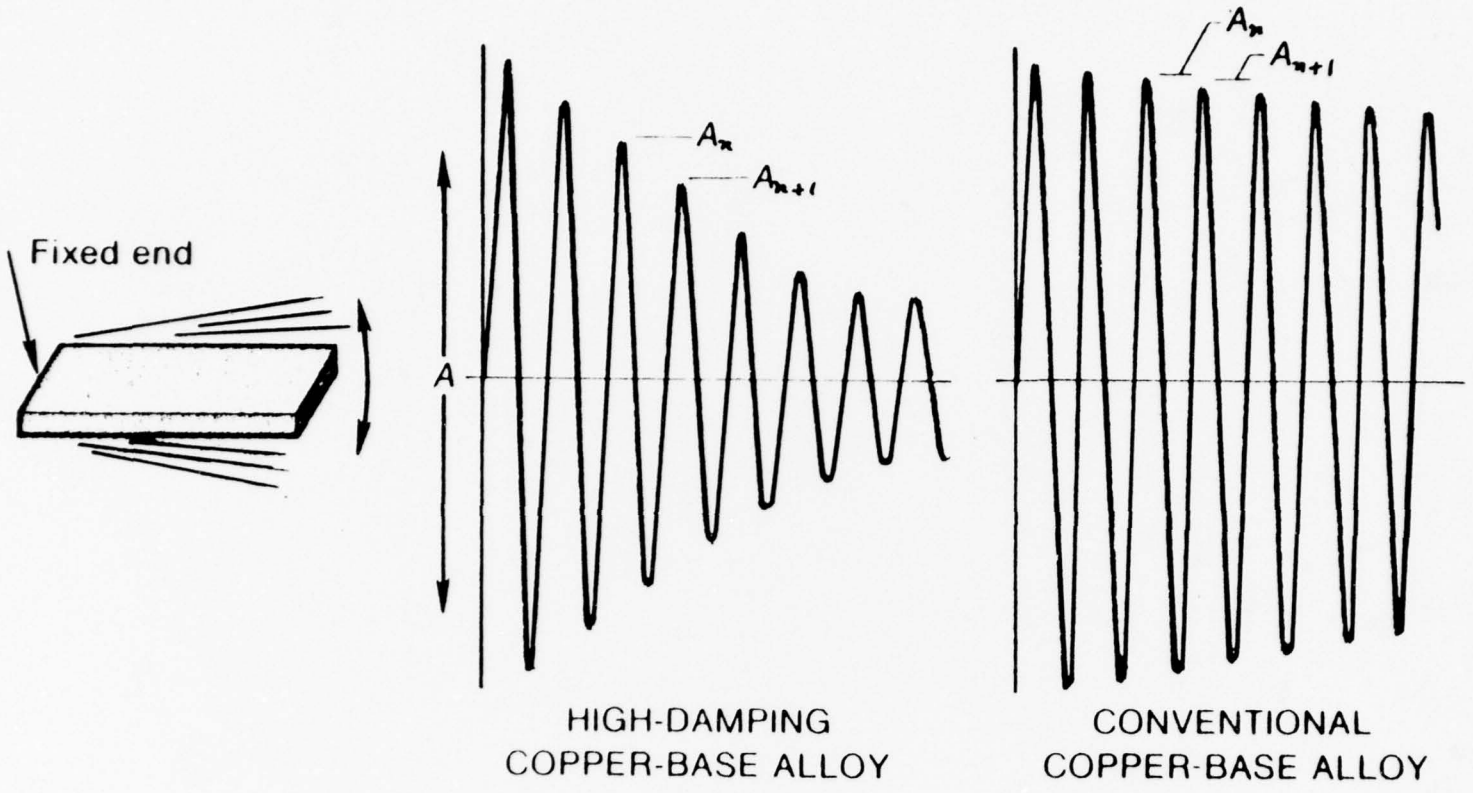

FIGURE 9. Experimental Method for Determining Specific Damping Capacity (Reproduced from Perkins [12])

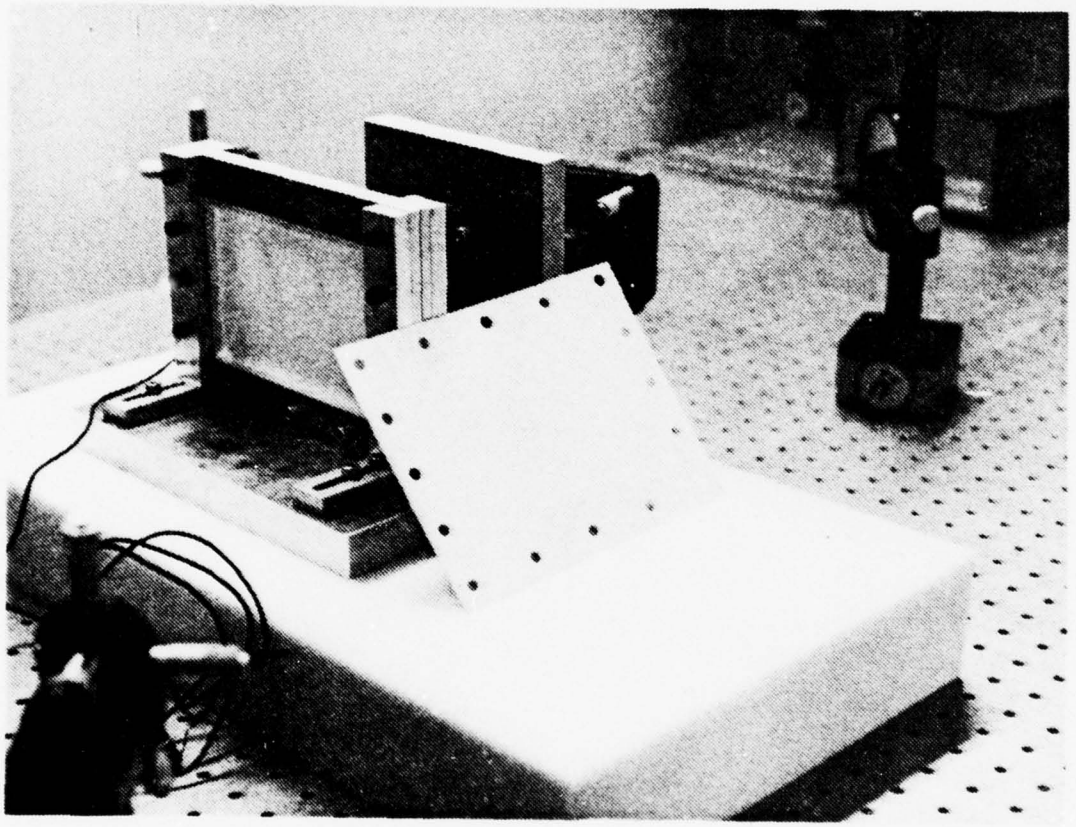

FIGURE 10. 2024-T4 Aluminum Test Specimen

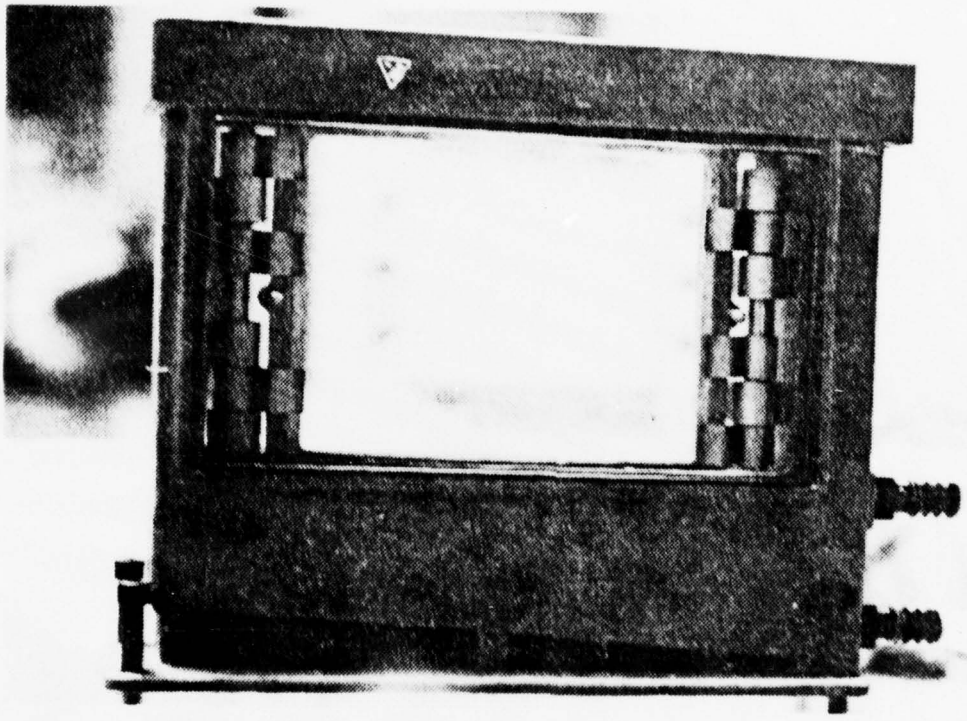

FIGURE 11. View Through the Plate Holder to the Test Specimen. When the Hologram Has Been Made it is Viewed Through This "Window."

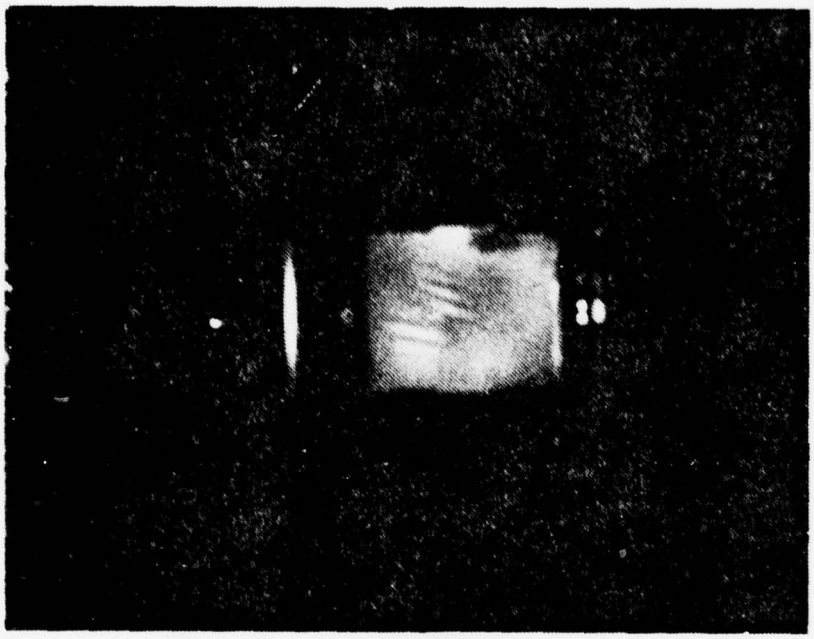

FIGURE 12. First Successful Hologram Reconstruction. This was Intended to be a Real-Time Hologram of the Plate. Fringes Indicate that Excessive Motion During the Exposure Made it a Time-Average Hologram. Specimen Mount was Removed from Foam Rubber and Bolted Down to Solve this Problem.

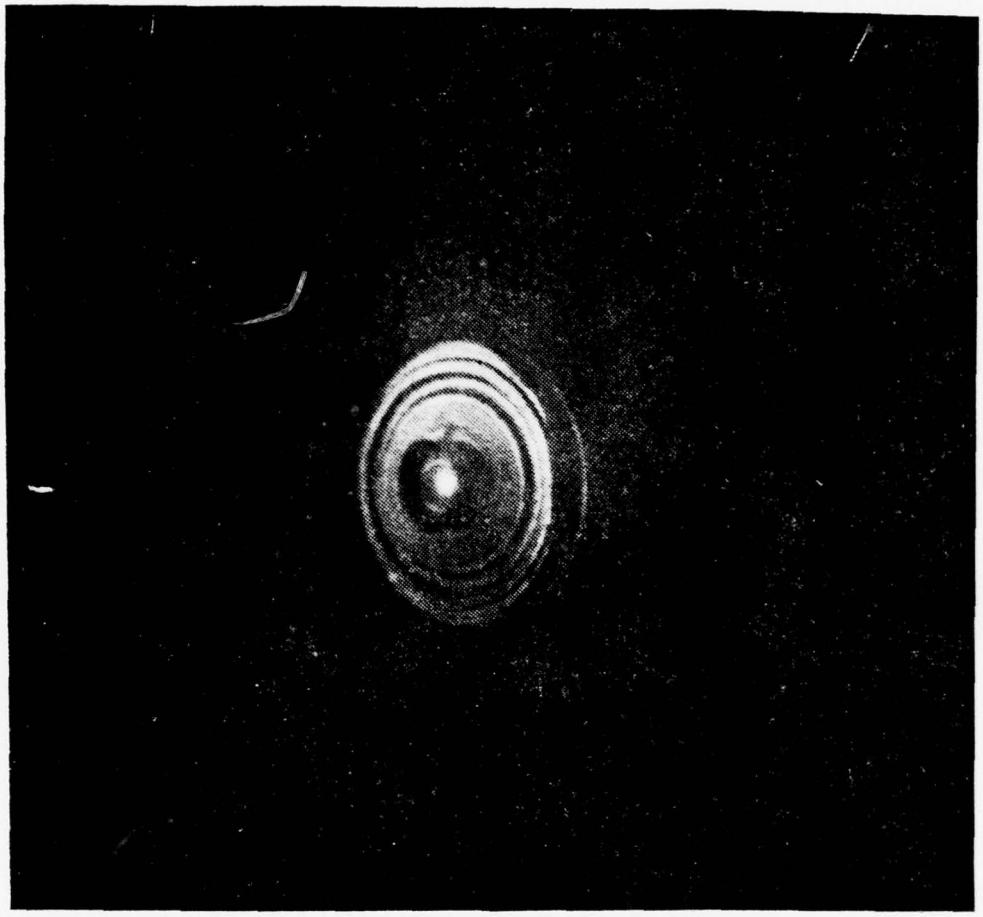

FIGURE 13. Real-Time Hologram of a Car Radio Speaker

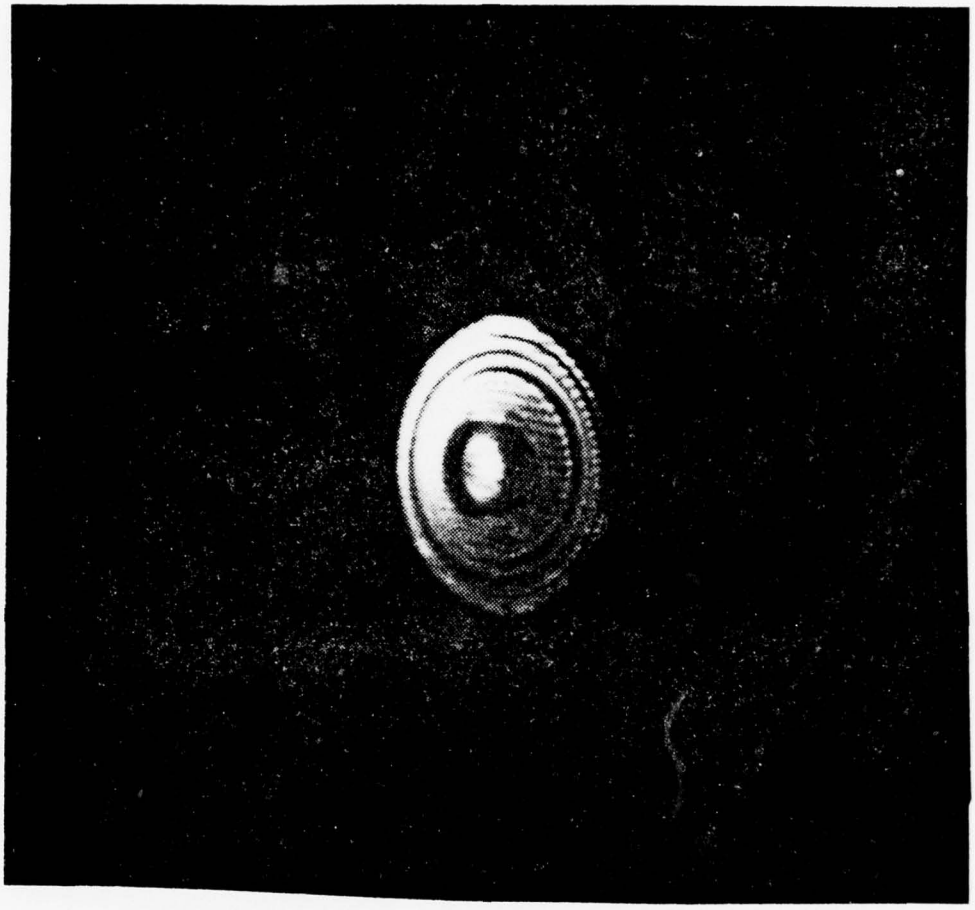

FIGURE 14. Real-Time Hologram of Car Radio Speaker Showing Fringes Caused by Gentle Taps on the Vice

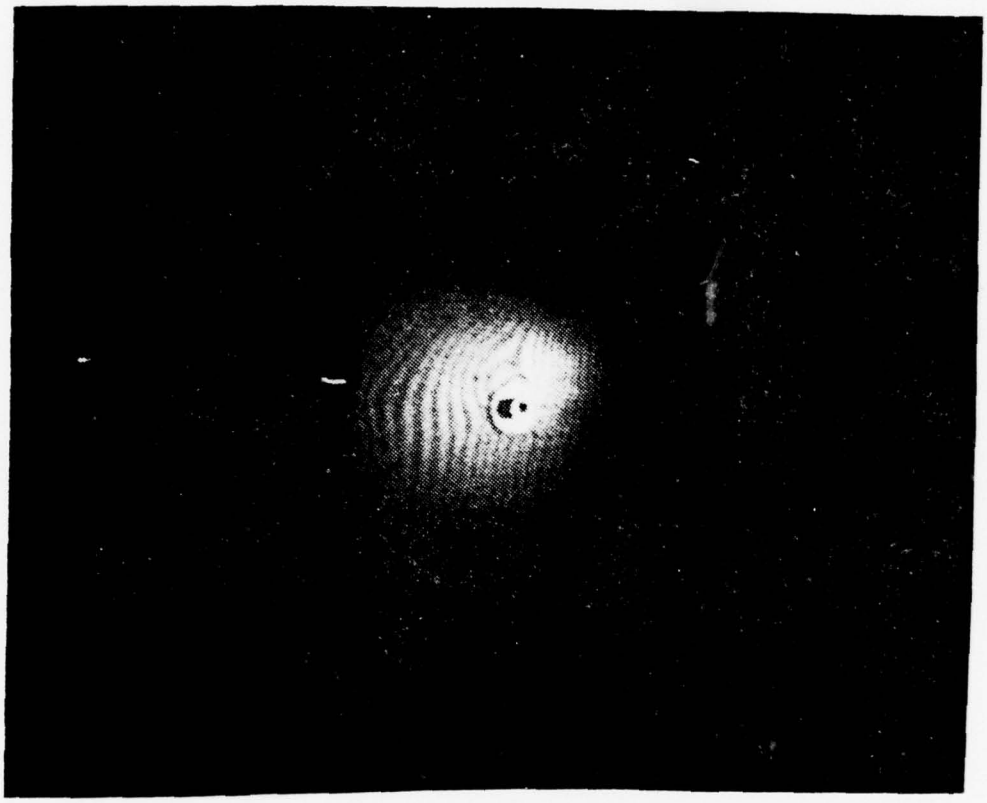

FIGURE 15. First Reconstruction of Plate Bolted to the Table. Fringes Indicate That Relative Motion Between the Mount and Photographic Plate has Occurred.

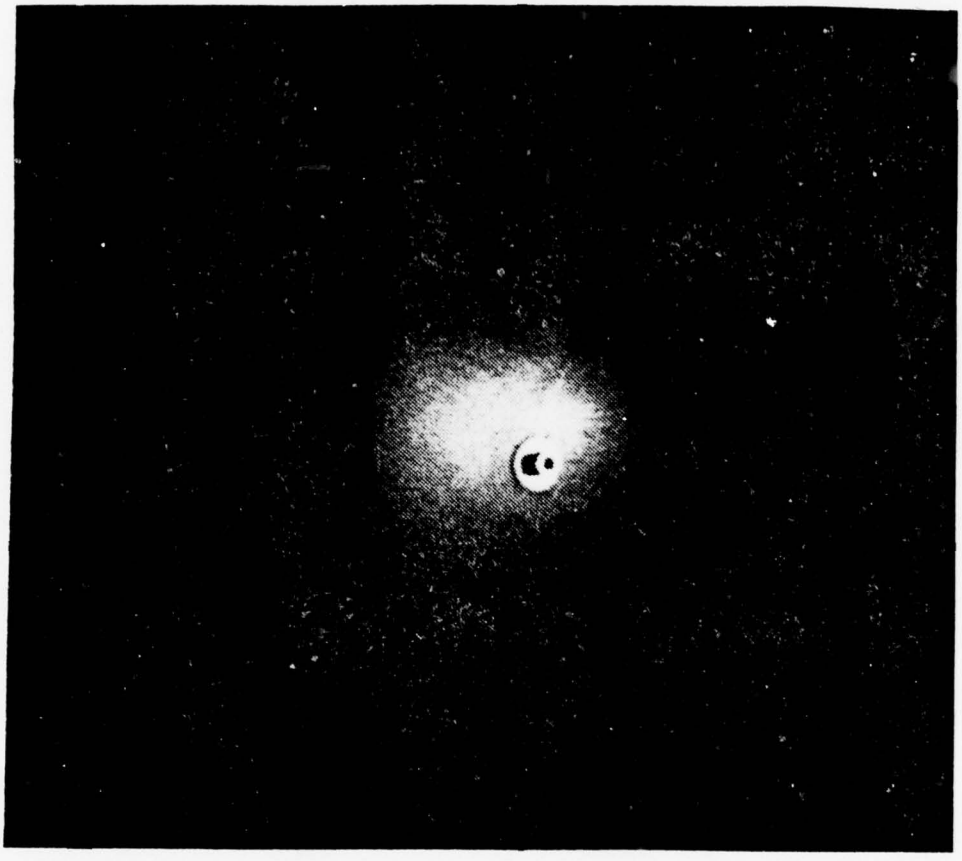

FIGURE 16. Test Specimen Vibrating in its Second Vibration Mode

FIGURE 17. Test Specimen Vibrating in its Fourth Vibration Mode

FIGURE 18. Second Vibration Mode of Plate Flowed with a Diagonal Slit

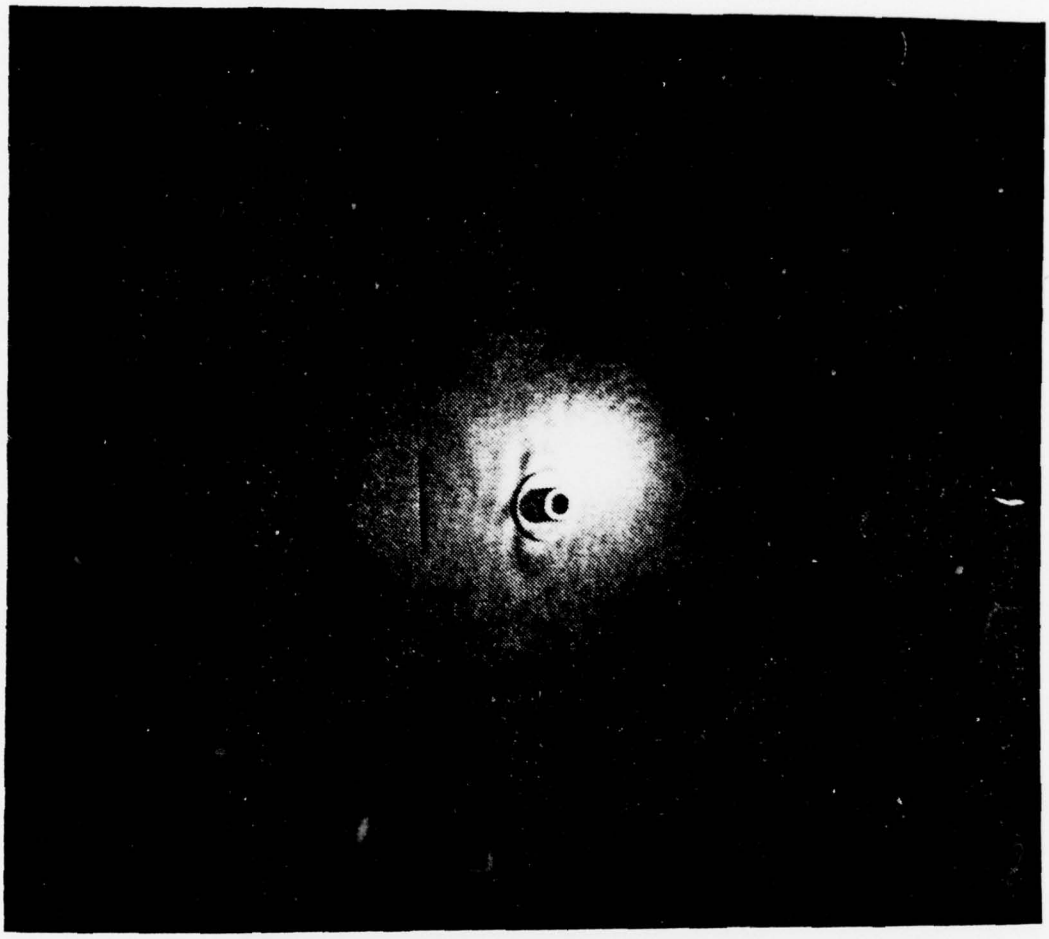

FIGURE 19. Second Mode Resonance in the Right Half of the Test Plate Flawed with a Vertical Slit

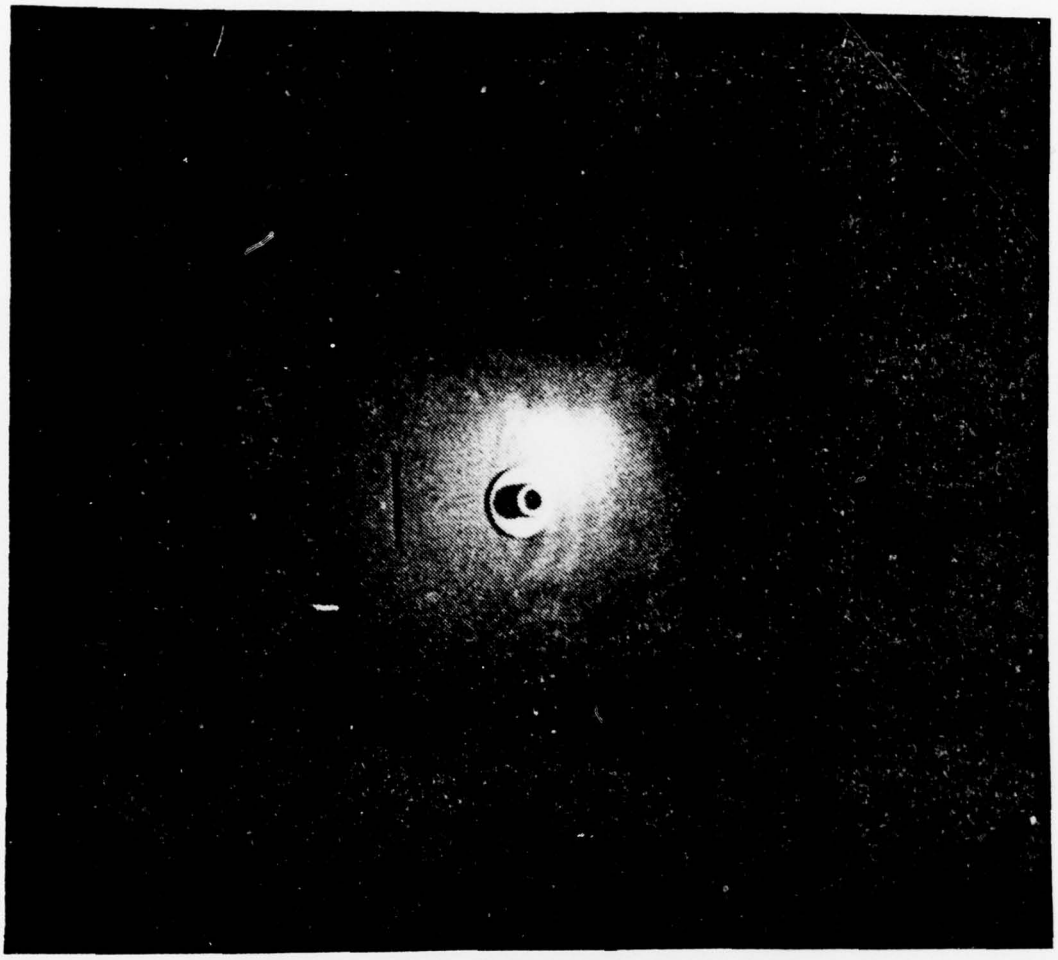

FIGURE 20. Second Mode Resonance in the Left Half of the Test Plate Flawed with a Vertical Slit

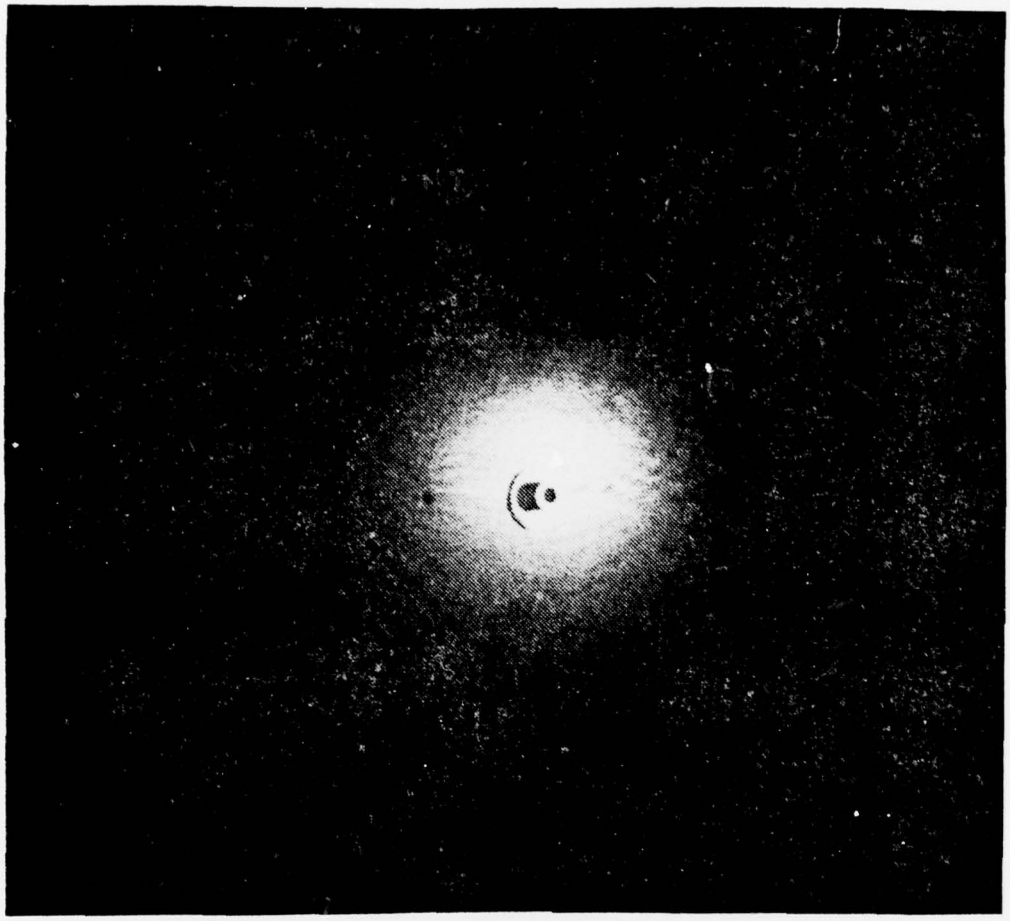

FIGURE 21. Fourth Mode Shape of the Test Plate Flawed with a Small Circular Hole

MATERIAL	SDC (%)
Magnesium (wrought)	49
Iron	16
Grey Cast Iron	6
Austenitic Stainless Steel	1
Aluminum Alloy 2024-T4	< 0.2

Table I. Specific Damping Capacities of Structural Materials

MODE (a)		RESONANT FREQUENCY (HZ)				
		WITHOUT FLAW		DIAGONAL SLIT	VERTICAL SLIT	CIRCULAR HOLE
n	m	THEORY	EXPERIMENT			
1	1	326.975	380.1			
1	2	814.407	630.8	615.1	563.2 (b) 510.1 (c)	588.8
2	1	987.829				
2	2		987.6	936.3		903.5

(a) See Leissa, Ref. [10], for definition of n and m

(b) Resonant frequency of portion of plate without slit

(c) Resonant frequency of portion of plate with slit

Table II. Summary of Resonant Frequencies

APPENDIX A

In order to provide some insight into the complications involved in theoretically predicting the resonant frequencies of the plate coupled to the piezoelectric driver, the following discussion from references [3] and [13] is provided.

First, a piezoelectric driver can be mathematically analyzed as follows:

Hooke's Law states that there exists a linear relationship between stress and strain. Let

T = stress tensor

S = strain tensor

C_{ij} = elastic compliance coefficients

Then

$$T_i = C_{ij}S_j \quad \text{(double subscripts imply summation)} \tag{A-1}$$

and

$$S_j = d_{kj}E_k \tag{A-2}$$

where E_k = kth component of electric field

d_{kj} = piezoelectric coefficients.

Expanding,

$$S_1 = d_{11}E_1 + d_{21}E_2 + d_{31}E_3 \tag{A-3}$$

but $E_2 = E_3 = 0$, so

$$S_1 = d_{11}E_1 \tag{A-4}$$

Note that fringing electric fields are neglected.

Substituting,

$$T_i = C_{ij}d_{kj}E_k \tag{A-5}$$

where $E = V/\ell$ [See Figure 22.] The voltage supplied to faces a and b is V. Spacing of faces a and b is ℓ. Then expanding,

$$T_i = C_{11}d_{11}E_1 + C_{12}d_{12}E_1 + C_{13}d_{13}E_1$$

Define $K = C_{1k}d_{1k}$ (A-6)

Therefore,

$$T_1 = KE_1 = KV/\ell \tag{A-7}$$

Now, there exists an analogy between the mechanics of a spring mass system and an electrical circuit. This mechanical analogy, which is apparent from equations (A-8) and (A-9), is used to obtain the model of a piezoelectric driver shown in Figure 23.

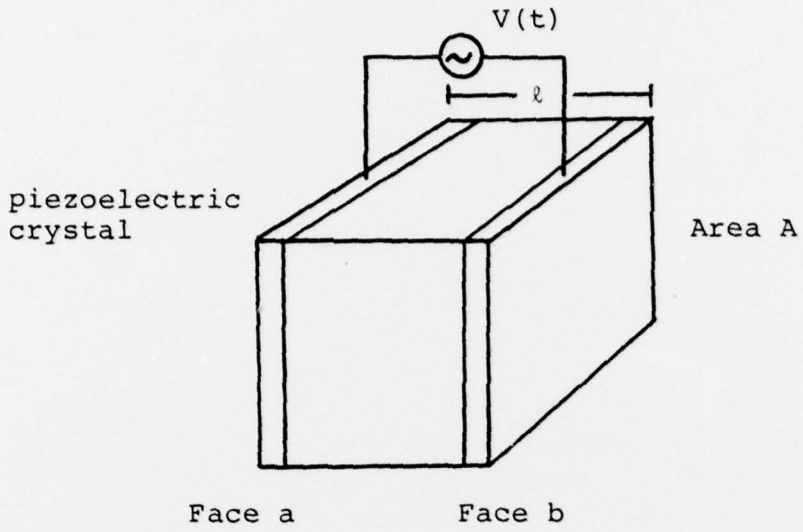

FIGURE 22. Piezoelectric Crystal

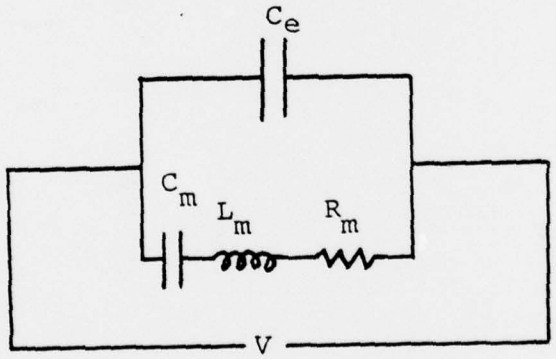

C_e = electric capacity
C_m = mechanical stiffness of crystal
L_m = mechanical mass of crystal
R_m = viscous damping within crystal

FIGURE 23. Model of a Piezoelectric Driver

$$L \frac{d^2i}{dt^2} + R \frac{di}{dt} + C^{-1}i = \frac{dV}{dt} \qquad \text{(A-8)}$$

$$m \frac{d^2x}{dt^2} + \beta \frac{dx}{dt} + kx = F(t) \qquad \text{(A-9)}$$

When a piezoelectric driver is used to drive a spring mass system, the system can be modelled as shown in Figure 24.

There are now four simultaneous equations, (A-10), (A-12), (A-13), and (A-14), which must be solved:

$$m \frac{d^2x}{dt^2} + \beta \frac{dx}{dt} + kx = F \qquad \text{(A-10)}$$

The force F is obtained from the stress in the crystal

$$F = T_1 A = kVA/\ell \qquad \text{(A-11)}$$

The relevant strain in the crystal is

$$S_1 = (\ell - x)/\ell = d_{11}V/\ell \qquad \text{(A-12)}$$

$$L_m \frac{d^2i}{dt} + R_m \frac{di}{dt} + C_m^{-1}i = \frac{\dot{Q}}{C_e} = \frac{dV}{dt} = -\frac{1}{d_{11}} \frac{dx}{dt} \qquad \text{(A-13)}$$

$V = d_{11}^{-1}(\ell - x)$ = oscillator voltage.

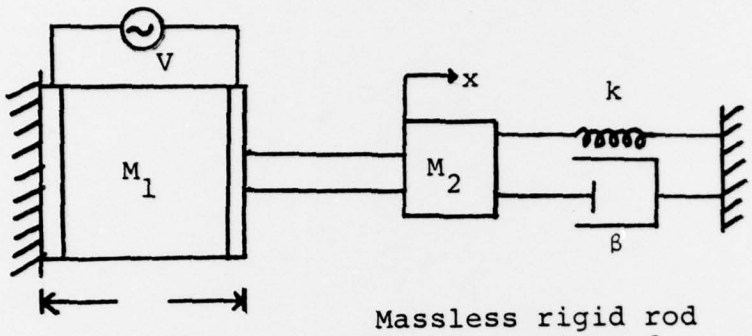

Massless rigid rod
F = force in rod
V(t) = drive voltage
of oscillator

FIGURE 24. Model of a Spring Mass System Driven by a Piezoelectric Driver

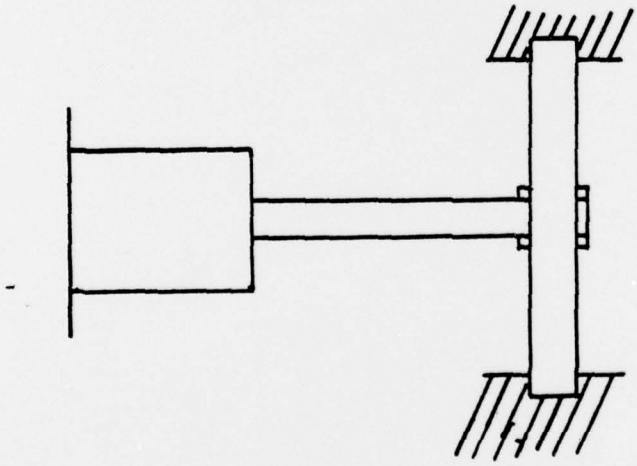

FIGURE 25. Model of Test Plate Being Driven by a Piezoelectric Shaker

In equation (A-13), Q is equal to the charge on C_e and $\dot{Q} = i$.

In order to model the plate coupled to the piezoelectric driver, Figure 25, work beyond the scope of this thesis would be required. Even so, the model of Figure 24 would provide considerable insight into this problem.

LIST OF REFERENCES

1. Baines, H., The Science of Photography, p. 133-134, Fountain Press, 1958.

2. Burckhardt, C. B., Collier, R. J., and Lin, L. H., Optical Holography, p. 418-426, Academic Press, 1971.

3. Condon, E. V., and Odishaw, H., Editors, Handbook of Physics, McGraw Hill Co., 1958.

4. Dainty, J. C. and Shaw, R., Image Science, p. 12-14, 46, Academic Press, 1974.

5. Develis, J. B. and Reynolds, G. O., Theory and Application of Holography, p. 1-5, Addison Wesley, 1967.

6. Edwards, G. R., Perkins, J., and Hills, N., Materials Approaches to Ship Silencing, Naval Postgraduate School, Monterey, California, 1974.

7. Erf, R. K., Editor, Holographic Nondestructive Testing, Academic Press, 1974.

8. Huber, P.M., Holographic Nondestructive Testing of Pipes, MSME Thesis, Naval Postgraduate School, Monterey, California, 1978.

9. Kock, W. E., Engineering Applications of Lasers and Holography, p. 59-65, 77-84, Plenum Press, 1975.

10. Leissa, A. W., Vibration of Plates, p. 58-65, National Aeronautics and Space Administration, 1969.

11. Mechanical Engineering Science, Monograph No. 1, The Forced Vibration of Circular Flat Plates, by A. J. McLeod and R. E. D. Bishop, March 1965.

12. Perkins, J., and Schetsky, L. M., "The 'Quiet' Alloys," Machine Design, p. 202-203, 6 April 1978.

13. Yu, F. T. S., Introduction to Diffraction, Information Processing and Holography, p. 338-341, MIT Press, 1973.

14. Von Hippel, A. R., Dielectrics and Waves, Chapter 26, Wiley, 1954.

INITIAL DISTRIBUTION LIST

		No. Copies
1.	Defense Documentation Center Cameron Station Alexandria, Virginia 22314	2
2.	Library, Code 0142 Naval Postgraduate School Monterey, California 93940	2
3.	Department Chairman, Code 69 Department of Mechanical Engineering Naval Postgraduate School Monterey, California 93940	1
4.	Professor A. E. Fuhs, Code 69Fu Department of Mechanical Engineering Naval Postgraduate School Monterey, California 93940	2
5.	LCDR Paul M. Huber, USN Portsmouth Naval Shipyard Portsmouth, N.H. 03801	1
6.	Commander Boston Naval Shipyard ATTN: Code 130 Boston, Massachusetts 02129	1
7.	Commander Puget Sound Naval Shipyard ATTN: Code 130 Bremerton, Washington 98314	1
8.	Commander Charleston Naval Shipyard ATTN: Code 130 Naval Base Charleston, South Carolina 29408	1
9.	Commander Long Beach Naval Shipyard ATTN: Code 130 Long Beach, California 90801	1
10.	Commander Pearl Harbor Naval Shipyard ATTN: Code 130 Box 400 Pearl Harbor, Hi 96860	1

11. Commander 1
Philadelphia Naval Shipyard
ATTN: Code 130
Philadelphia, Pennsylvania 19112

12. Commander 1
Portsmouth Naval Shipyard
ATTN: Code 130
Portsmouth, New Hampshire 03801

13. Commander 1
Norfolk Naval Shipyard
ATTN: Code 130
Portsmouth, Virginia 23709

14. Commander 1
Mare Island Naval Shipyard
ATTN: Code 130
Vallejo, California 94592

15. *LT. Phil Hoffmann, USN* 2
Class 4-78B
Engineering Duty Officer School
Mare Island
Vallejo, Ca 94592

16. *CAPT. Alfred Skolnick* 1
Naval Sea Systems Command
PMS 405
Crystal City
Washington, D.C. 22202

17. RADM. James W. Lisanby 1
Naval Ship Engineering Center
NAVSEA 6000
N.C. 2 Crystal City
Washington, D.C. 22202